Computational and Theoretical Chemistry 1115 (2017) 335–343

Contents lists available at ScienceDirect

Computational and Theoretical Chemistry

journal homepage: www.elsevier.com/locate/comptc

Weak bonds between molecular tweezers and their guests

Marlene Bosquez, Alejandra Cambray, Alan Miralrio, Roxana-Mitzayé del Castillo, Roberto Salcedo *

Instituto de Investigaciones en Materiales, UNAM, Circuito exterior s/n, ciudad universitaria, 04510 Coyoacan, Mexico City, Mexico

ARTICLE INFO

Article history:
Received 8 May 2017
Received in revised form 28 June 2017
Accepted 13 July 2017
Available online 14 July 2017

Keywords:
Tweezers
Metallocenes
Nanotubes
Nanotori

ABSTRACT

It is proposed a molecular tweezer, which makes possible to design a scaffold structure, allowing to trap organic molecules, regardless of the size of the guest. Weak carbon-carbon and carbon-hydrogens interactions stabilized the compound. The analysis carried out with the Grimme's dispersion correction allow to quantify the weak interaction between the molecular tweezer and the guest. These assumptions were confirmed into the framework of quantum theory of atoms in molecules, due to the existence of bond critical points connecting carbon and hydrogen tweezer's atoms and carbon atom of the guest species. The density of states shows that it is possible to observe that the only contribution near the active regions is made by the guest species. The tweezer molecule is the perfect host for organic molecules, because there is no electronic interaction between them. The electronic properties of the guest species remains unchanged under the molecular tweezer interaction.

1. Introduction

Molecular tweezers [1–3] are organic systems (predominantly aromatic) that can be twisted in such a way that they adopt the shape of a claw. This generates a cavity, where it is possible propose a guest occupying the cavity, which is able to establish interactions with the host. Tweezers can take a number of forms, Fig. 1 presents some examples [4–6].

In Fig. 1, it is possible observe structures with aromatic rings at the ends. The aromatics rings at the end make possible that the π electron cloud could interact with different chemical entities, making these structures more viable for experimental designs [7,8].

Aromatic rings can form organometallic complexes by linking with metal atoms and this feature involves coordinated covalent bonds, which can also form very large arrangements by means of π-π stacking or even generate communications through space, as in nucleic acids [9]. However, most importantly, many of these cases correspond to supramolecular interactions that are able to produce different molecular complexes, suitable for a wide variety of applications [10].

It is important to emphasize the large relevance of this kind of molecules because molecular tweezers are receptors of other kind of molecules and this activity has been studied in experimental as well as theoretical works [1,11]. In particular the theoretical research can contribute in important manner because the development of new methods can help to explain the nature of weak bonds [12] and the considerable influence of them in the supramolecular interactions which experiments the tweezers and their guests.

In this sense it is important to mention works as those of Martin [13], Denis [14] and Truhlar [15] which have theoretically studied the interaction of some tweezers and fullerenes, the study of Jacquemin [16,17] about the capture of aromatic molecules by means tweezers and the evaluation of the trapping power of these systems reported by Tkatchenko [18], all these works are important contributions to the study of weak interactions, but furthermore they contribute to design new chemical systems which can have utility in different fields of study which can be energy, pharmaceutical or catalysis.

Nanotubes are allotropes of carbon which can be considered as cylindrical arrangements of graphene sheets [19]. These can be either single or multiple walled and can present multiple diameters. The nature of the walls is closely related to the aromaticity of their single rings, i.e. the π-electrons are positioned to interact with other organic species.

The initial idea to form a complex between nanotubes and tweezers was published in 2008 [20,21]. This conceived a large diameter nanotube associated with pyrene-tetrathiafulvalene, and here the idea was to have a kind of staple to help with the immobilization of the nanotube.

The present work deals with a theoretical study about the interactions between molecular tweezers that work as a scaffold, and different guests such as chromium atoms or narrow nanotubes. There are different types of bonds, the nature of these bonds are discussed here

* Corresponding author.
E-mail address: salcevitch@gmail.com (R. Salcedo).

http://dx.doi.org/10.1016/j.comptc.2017.07.010
2210-271X/

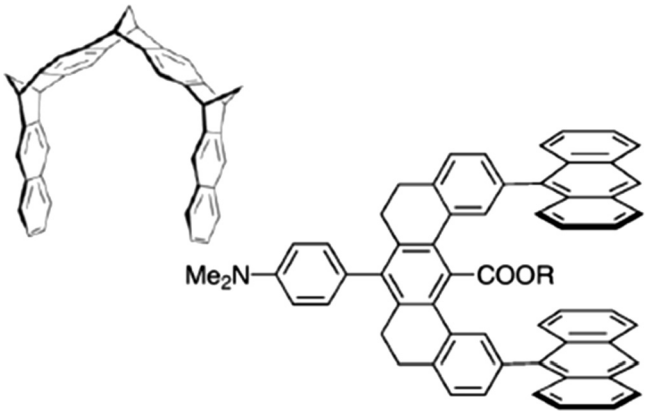

Fig. 1. Examples of molecular tweezers.

2. Methods

The optimization process of all designed species was carried out in two stages. Firstly, the computational chemistry software NWChem [24] was used to carried out a 10,000 stage Molecular Mechanic conformational search using Amber force field with the Amber parameter set [22,23], in order to achieve the global minimum, all NWChem default parameters were used. Secondly, as implemented in the Gaussian09 package [25] the highly parametrized functional meta-GGA of Truhlar and Zhao named M06-L [26,27] was used to optimize all geometries and in all calculations, the 6-31G** basis set was used for all atoms. A further comparison with the larger basis set 6-311G** was carried out for a chromium containing complex. The basis 6-31G** was used in order to save computational resources, giving comparable results to the larger basis set, details below.

Grimme's empirical dispersion corrections [28] (D3) were used for calculate the energy due to weak interactions (London dispersion forces) between molecular tweezer and hosted species. That scheme has been used satisfactorily since its original formulation to quantify the dissociation energies in van der Waals complexes as a "bucky ball catcher" hosting a fullerene C_{60}.

Those calculations were carried out using the DFT-D3 stand alone code provided by Grimme [28], which provides the correction to the total electronic energy (calculated at the DFT level M06-L/6-31G**) in addition to separate intra and intermolecular weak interactions. The M06-L functionals is claimed to capture "medium-range" interactions [29], meanwhile our Grimme analysis consider part of the large distance interactions. With the combination of both methods, it is enough to have a quantitative analysis of the interaction between the hosted species and the molecular tweezer.

In comparison to experimental measures obtained for several organic van der Waals complexes, dispersion-corrected methods have proven to improve the results obtained with uncorrected functionals [30] including highly parametrized functionals as the family M06 [31]. Overall, include a correction to the energy as the proposed by Grimme is necessary to study complexes which involve weak interactions, apart from the DFT functional chosen.

The convergence threshold used in the present paper are the threshold default given in the Gaussian09 package; scf convergencia criteria is 10^{-8} a.u.; and RMS force criterion is 10^{-4} a.u.

The density of states of the total system (TDOS) has been calculated using the MULTIWFN computational package [32]. In order to achieve the TDOS for isolated systems, the TDOS is extrapolated with a Gaussian function $G(x)$:

$$G(x) = \frac{1}{c\sqrt{2\pi}} e^{\frac{x^2}{2c^2}},$$

In which $c = \frac{d}{2\sqrt{2\ln 3}}$, d is an adjustable parameter which represent the full width at half maximum. The Fermi energy is determined as the middle point of the band gap $E_F = \frac{(E_{LUMO} - E_{HOMO})}{2}$. It is also shown the contribution in the density of states of each compound (Tweezer and Nanotube/Nanotori) of the whole system, which is called as the partial density of states (PDOS). The PDOS for the fragment A is calculated as

$$PDOS_A(E) = \sum_i \Xi_{i,A} G(E - \varepsilon_i),$$

where $\Xi_{i,A}$ is the composition of the fragment A in the orbital i. The composition of the fragment A is estimate with Mulliken charge analysis. To estimate the DOS is necessary to include the option "pop = full" in the optimization input, in specific in the G09 input.

3. Results and discussion

3.1. Molecular tweezer metallocene

In Fig. 2a, it is shown the empty tweezer molecule (molecule **1**). In Fig. 2b, it is shown the tweezer molecule with an anthracene complex as guest, this structure is entitled as molecule **2**. In Fig. 2c, it is shown the tweezer molecule with an anthracene π complex and four chromium atoms as guest.

The election of chromium as the guest of the tweezer has its source in the nature of the bis-dibenzene-chromium compound [33] in which two benzene rings can interact with a chromium atom in oxidation state 0, therefore the resultant species can be studied considering it as a large example of a metallocene, the inclusion of other transition metals will be the theme of a future research work. The structure can be studied including four or six metal atoms which can interact with the aromatic rings of the tweezer and also with those of the anthracene guest, however the species containing six atoms shows large difficult to optimize, perhaps the regions is so crowded in electronic traffic, however the species containing four was easily optimized and this was the cornerstone of this part of the study. Therefore the whole compound shows a charge of 0. Respect the multiplicity, several other calculations were performed looking for stable large multiplicity states because in particular chromium exhibits the tendency to delocalize several electrons, however no other multiplicity state reach stable configuration.

The molecule **1** belongs to a C_2 point group symmetry; the average distance between arms is 8 Å. The hollow molecular tweezer (molecule **1**) shows three electron rich regions; the lateral bridge; and the both arms of the molecular tweezer. This behavior can be appreciated in the schemes of the frontier molecular orbitals (MO's) shown in Fig. 3. The size and shape of the three main regions suggest that there exist limited or null communication between them. Likewise, the energy gap (HOMO-LUMO gap) between these functions is 5.36 eV or 123.28 kcal/mol, placing this species in the category of insulator. According with previously mentioned, the communication should be established by the formation of inclusion complexes, In addition to the possibility of adjust the energy gap.

The formation of this type of inclusion complex has been suggested previously [1,5]. Molecule **2** is an example where an anthracene molecule is placed in the cleft between both arms, reaching the minimum energy structure. The included anthracene species is not localized at a completely symmetric position with respect to the arms of the tweezer (see Fig. 4), therefore the distances between the corresponding carbon atoms vary around an average

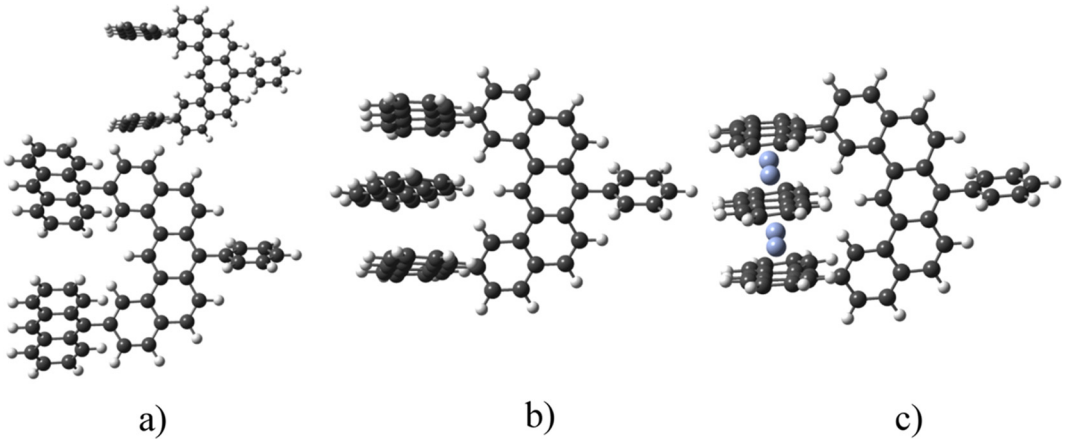

Fig. 2. (a) Two different views of the tweezer molecule without interactions (molecule **1**). (b) The inclusion complex (molecule **2**) of anthracene and molecule **1**. (c) The same tweezer molecule containing a new anthracene molecule and four chromium atoms (molecule **3**).

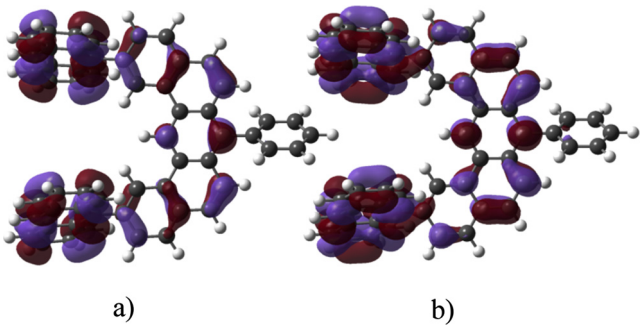

Fig. 3. Frontier molecular orbitals of molecule **1**: (a) HOMO and (b) LUMO.

value of 3.93 Å, this distance suggests Van der Waals interactions (VdW). The dispersion forces between the molecular tweezer and anthracene were calculated as −0.52 eV or −12.42 kcal/mol.

The frontier molecular orbitals in this case manifest important differences compared to the hollow molecular tweezer **1**. These are presented in Fig. 4.

Besides, it is possible to suggest a communication between the three decks, although functions do not overlap. The orbitals are, spatially, closer than the empty case and the value of the energy gap in this case is 2.31 eV or 53.13 kcal/mol, clearly indicating a gap, characteristic of a semiconductor species.

Another possibility would be to attach aromatic guests by using a stronger kind of bond, i.e. using a bond that coordinates with a metal or several metal centers. This feature would imply the formation of an organometallic complex, precisely in the form of molecule **3**. The complex 3 is built from the framework of molecule **1** [5], an anthracene molecule and four atoms of chromium with oxidation state zero; this is an example of a large metallocene **3**. The important point is that this complex has a triple decker π system, which resembles a multiple bis-benzene-chromium. The corresponding molecular orbitals diagram appears in Fig. 5, where remarkably, the molecule does not belong to any symmetry group, (indeed the region of the dibenz[*a*,*f*]anthracene shows a slight curvature out of the plane of the planar cycles). However it has a very marked double set of degenerated orbitals that form the HOMO and HOMO−1 functions, (with a difference in energy of 0.03 eV or 0.69 kcal/mol very close to each other); the first one with two molecular orbitals and the second one with three, which is obviously a case of accidental degenerated MO's. The existence of this set of molecular orbitals is not expected for this group of symmetry, although it is reminiscent of the metallocene moiety (because the bis-benzene-chromium shows a similar distribution [33]), as this allocates all its electronic interactions. The entire orbitals (HOMO and HOMO−1) are found on the electronic delocalized organic region and the d atomic orbitals of the metal atoms.

In another context, the LUMO is a single molecular orbital which encompasses the π anti-bond interaction between chromium atoms and the aromatic rings. Notably, the presence of the electronic richness of the HOMO causes the LUMO to approach with a related narrowing in energy. It is thus possible to recognize the HOMO-LUMO energy gap of 0.353 eV or 8.119 kcal/mol, which means that this compound will be a strong semiconductor or a moderate conductor.

The bond comprises a classical π interaction, similar to that shown in bis-benzen-chromium (bbCr). The compared bond lengths (average) help to reveal the geometry of the compound and in Table 1 considering comparison of bis-benzene-chromium [34] and chromium anthracene complex $Cr_2(Ant)_2$ [23] is made.

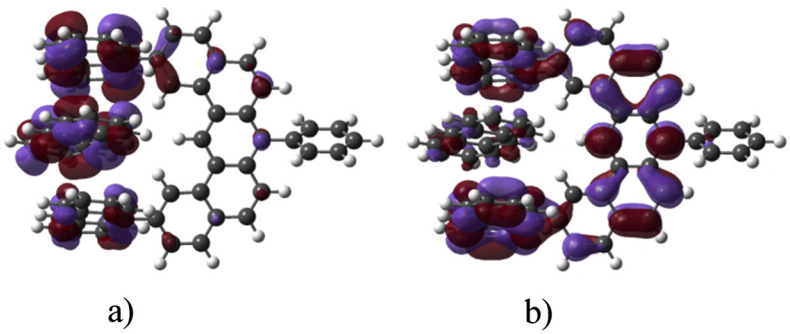

Fig. 4. Frontier molecular orbitals of molecule **2**: (a) HOMO and (b) LUMO.

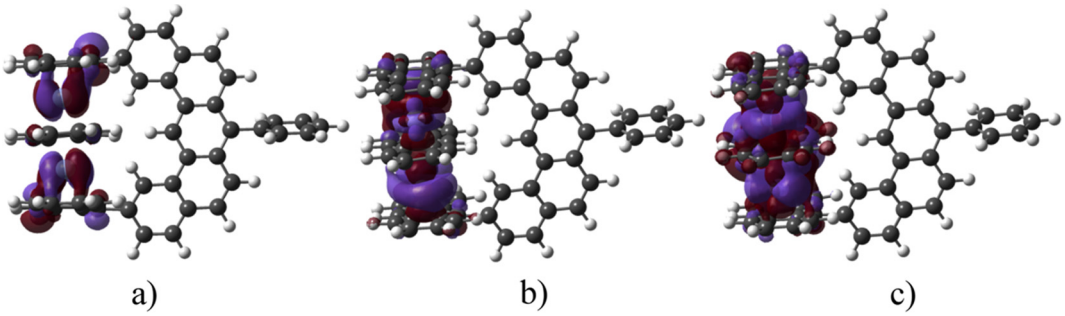

Fig. 5. Frontier molecular orbitals of complex **3**: (a) LUMO, (b) HOMO and (c) HOMO−1.

Table 1
Selected bond lengths of complex 3, bbCr and $Cr_2(Ant)_2$. For comparison, values calculated at the M06-L/6-311G** level in parentheses.

Bond length	Compound		
	Complex 3	bbCr	$Cr_2(Ant)_2$
M—C	2.139 (2.118)	2.142	2.281
C—C	3.358 (3.401)	3.220	3.508

This reasonably small system containing the heaviest element in the present work allow to compare the results of the chosen basis set with the larger 6-311G** basis set. Table 1 shows that the bond lengths calculated at both levels are pretty comparable between them as well as the bis-benzene-chromium and chromium anthracene complex. As well, comparing energy levels the results are similar. The HOMO-LUMO gap of 0.219 eV or 5.037 kcal/mol calculated at the M06-L/6-311G** level is comparable to the 0.353 eV or 8.119 kcal/mol obtained with the method chosen. Similarly, the energy difference between HOMO and HOMO-1 was calculated as 0.05 eV//1.15 kcal/mol, similar to the 0.03 eV or 0.69 kcal/mol calculated at the other level. Thus, the basis set 6-31G** was enough to study this system and offer a cost-benefit relationship suitable to study the following systems which consist of hundred of atoms.

Two interesting points emerge; firstly, it has been suggested that compounds such as molecule **1** will be effective catchers of sole aromatic rings, a fact shown to be true, because of the formation and thermodynamic stability of compound **2**. However the intrinsic geometry and stabilization of molecule **3** shows that the tweezer can also produce a metallocene type compound. Secondly, the dimensions shown in Table 1 suggest that **3** is a compound with characteristics ranging between the bis-benzene-chromium and an anthracene chromium complex.

3.2. Tweezer as scaffold

It has been suggested that tweezer type molecules can serve as molecular scaffolds [35]. The possibility of having "fixed" nanotubes or other nanostructure fragments trapped into the cleft of a molecular scaffold has also been achieved [20,21,35], although in these cases the nature of the tweezer moiety is different to the present case. However it is important to emphasize that the experimental work carried out by both groups aimed to create a π-π stacking interaction molecule. The designed tweezers including the trapped nanotube are shown in Fig. 6.

The band structure of infinitely large carbon nanotubes has been approached satisfactory [36] through a π-only band theory, concluding that all carbon nanotubes with chiral vector (n,m) are metallic only if (n − m)/3 is an integer, and otherwise is a semiconductor. According with that, the infinitely large nanotube (5,5) is metallic [37] and (6,4) is semiconductor . The last one is a moderate semiconductor, with a band gap calculated ranging from 0.90 eV//20.7 kcal/mol [38] to 1.2 eV//27.6 kcal/mol [39]. It is remarkable that the properties can be substantially modified by varying the carbon nanotube length [40–42].

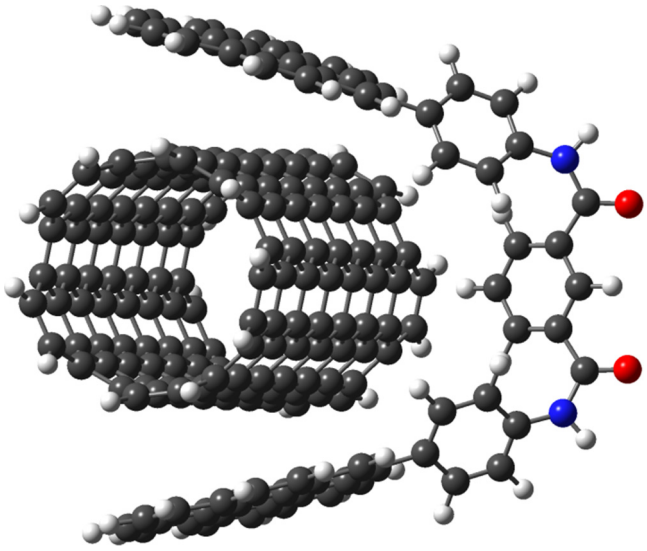

Fig. 6. Optimized structure of carbon nanotube (5,5) and molecular tweezer.

In order to study the interaction between carbon nanotubes and the tweezer in a molecular approach, we choose a finite carbon nanotube (5,5) and another one (6,4) with chemical formulae $C_{150}H_{20}$ and $C_{148}H_{20}$, respectively. Both have hydrogen atoms at the borders in order to complete the valence for all carbons. The designed tweezers including the trapped nanotube are shown in Figs. 6 and 9.

This was designed following some examples provided by Fukazawa and coworkers [43]. However in all cases presented in their work, the ends only present benzene rings or phenanthrene rings with no symmetrical ends, i.e., with different molecules at the ends. Contrastingly, in our case both ends are the same and they are both coronene, a molecule which was chosen because of its large aromaticity and the stock of 24 electrons in its delocalized cloud, which warrants interaction with other species.

The size of the cavity is 9.75 Å (measured between two equivalent carbon atoms from each deck). It is therefore possible to allocate a nanotube with a smaller diameter than this value (in this case it is a nanotube with chiral indices (5,5)), the appropriate species, it is shown in Fig. 6. It can be comfortably localized between the jaws of the tweezers having even more room to consider different kinds of bond (i.e. covalent or dispersion forces).

The resultant complex shown in Fig. 6 (molecule **4**) has an average distance between the surface of the nanotube and the planar carbon arrangement from the coronene of 3.35 Å, a value which

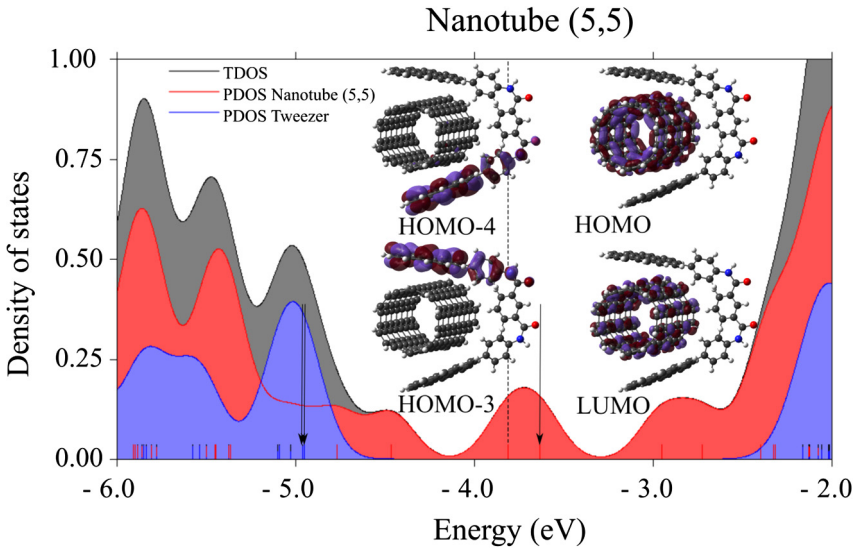

Fig. 7. Total and partial density of states and selected frontier orbitals of the scaffold complex (molecule **4**), dashed line indicates HOMO.

is very large for a covalent bond. However, it is sufficient to be described by Van der Waals forces. The interaction takes place between carbon atoms from both aromatic systems but this position is not the one which favors π-π stacking i.e. the one with eclipsed hexagons. Instead of this conformation, it appears that the carbon atoms undergo diagonal interactions in such a way that the confluence of three hexagonal rings on the coronene surface approximately coincides with the geometrical center of a hexagon at the nanotube surface. This result concurs with those in which the π-π interaction in the benzene dimer was studied [44,45]. Apparently here, the parallel displaced configuration is preferred to the sandwich one. The binding energy between the complex and their components was calculated as −2.41 eV//−55.34 kcal/mol. The total magnitude of the proposed Van der Waals forces is −1.33 eV//−30.47 kcal/mol. Assuming this to be so, the greater part of the binding energy results from the Van der Waals interaction between the tweezer and the nanotube (5,5).

The Molecular Orbitals scheme shows a very interesting situation. LUMO as well as HOMO, HOMO−1 and HOMO−2, all belong to the nanotube moiety; however the corresponding contributions coming from the jaws of the tweezers are revealed up to HOMO−3, HOMO−4 and HOMO−5 in an accidental degenerated set which is separated from the HOMO by only 1.14 eV//26.22 kcal/mol (Fig. 7). This means that it is possible to have weak bond relationships between both aromatic sets (i.e. the external wall of the nanotube and the arms of the tweezer).

Besides this, the energy gap between HOMO and LUMO is only 0.19 eV//4.37 kcal/mol which corresponds to a conductor species (typical behavior for this kind of nanotube). The significance of this aspect is transcendent because the chemical and physical characteristics of the nanotube molecule are reminiscent of the formation of the complex but occur in an immobilized structure.

In Fig. 7, it is presented the density of states of the tweezer molecule with a carbon nanotube of (5,5). The density of states presented in the present work, represents the energy levels of the isolated system with a Gaussian, reported in the Method section. It is shown in gray the TDOS, which is the total density of states of the compound. The red[1] line shown the partial density of states (PDOS) of the carbon nanotube (5,5). The blue line displays the PDOS of the tweezer molecule the energy gap is determined by the hosted species, according with the PDOS of the nanotube 5,5 (Fig. 7), where the energy levels around HOMO region are dominated, completely, by the nanotube's levels. The most remarkable thing to observe is that in the superposition of the PDOS, there is a region in which the carbon nanotube is the only entity that makes a contribution in the TDOS. This corresponds exactly with the MOs analysis already made. In Fig. 7, it is also shown some orbitals of the whole system. In the HOMO and LUMO orbitals, the only contribution at the MOs is made by the carbon nanotube, as it is possible

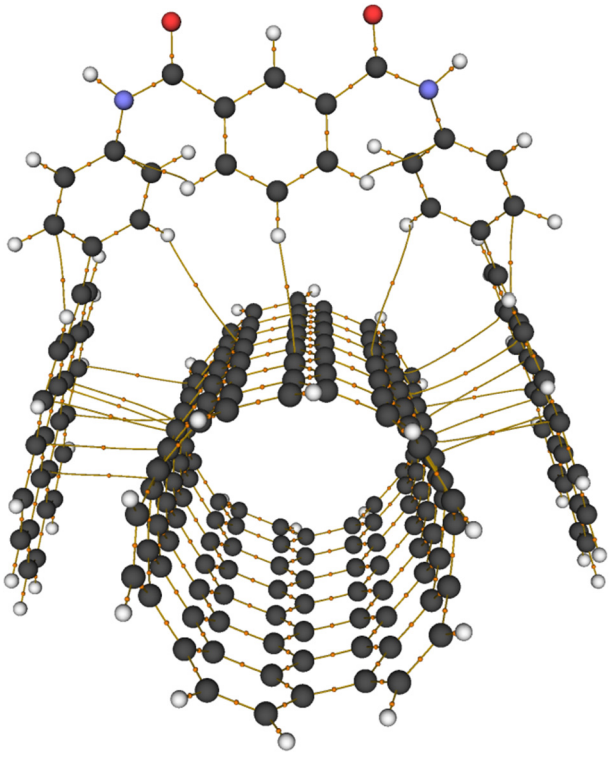

Fig. 8. QTAIM molecular graph of carbon nanotube (5,5) and molecular tweezer, orange dots are bond critical points. (For interpretation of the references to colour in this figure legend, the reader is referred to the web version of this article.)

[1] For interpretation of color in Figs. 7, 10 and 13, the reader is referred to the web version of this article.

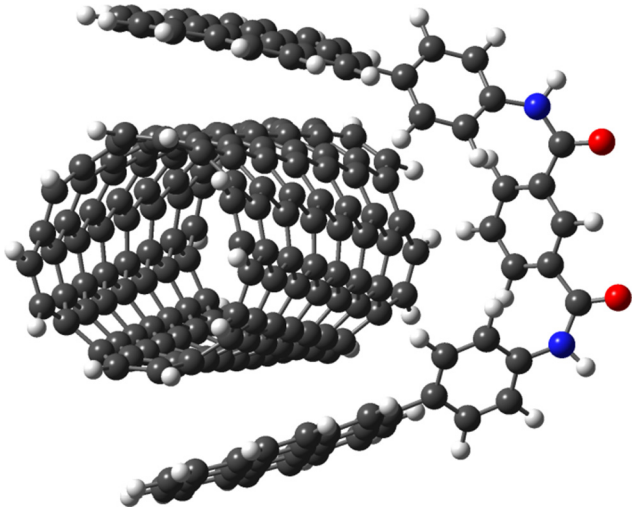

Fig. 9. The molecule being studied, optimized nanotube (6,4) and tweezer (molecule **5**).

to seeing in the TDOS (the red line is the only PDOS that made a contribution to the TDOS). This make that this tweezer molecule will be an excellent choice to trap complicated guests as carbon nanotubes maintaining its electronic properties mostly unchanged.

On the other hand, the quantum theory of atoms in molecules (QTAIM) has been used favorably in the analysis and determination of the formation of carbon-carbon and carbon-hydrogen weak interactions among several organic molecules [46–48]. The topology of the electron density of the following systems has been analyzed in order to show the weak interactions between the molecular tweezer and hosted species. These studies were carried out with the wavefunction obtained at the level of theory discussed previously. Bond paths (orange lines in the molecular graph) and bond critical points (orange dots in the molecular graph) have been found with the program of wavefunction analysis Multiwfn 3.6(dev) [32] to get the molecular graph on each case.

Furthermore, the low energy interactions were taking account 14 Van der Waals carbon-carbon bonds and 3 carbon-hydrogen bonds, these assumptions were achieved into the framework of QTAIM. According that theory, the presence of a bond critical point between two atoms interconnected by a bond path can be considered as a bond [46–48]. All these bonds are shown in Fig. 8 and the sum of all of these arrives at the number previously discussed.

A type of isomerism exists for single walled nanotubes. The species which appears in the figure corresponds (Fig. 6) to the classification of metallic nanotubes, but a proper isomer with (6,4) definition will correspond to the zig-zag nanotube classification and this should behaves as a semiconductor. This case was also considered in molecule **5** and is shown in Fig. 9. Here, it is evident that the energy levels and molecular orbitals are all very similar to that of molecule **4**.

Despite the semiconductor behavior of an infinitely large nanotube (6,4), the finite nanotube proposed has only 0.7 eV//13.1 kcal/mol of HOMO-LUMO gap, closing the gap. This difference may relate to the small length of our nanotube in comparison with the infinitely large nanotube (6,4) [39].

Considering molecule **5**, its molecular orbitals show a similar situation. LUMO as well as HOMO, HOMO−1 and HOMO−2 correspond to the nanotube. The contributions from the jaws of the tweezers are found up to HOMO−3 and HOMO−4, with small contributions on the wall of the nanotube (Fig. 10). The orbitals related to the tweezers appear 1.16 eV//23.68 kcal/mol deeper in energy than the HOMO.

Fig. 10 shows the density of states of the tweezer molecule with a carbon nanotube of (6,4). The gray line represents the total density of states of the system, meanwhile the red line reproduced the PDOS of the carbon nanotube (6,4) and the blue line is the PDOS of the tweezer molecule. Once again, it is possible observed that the only contribution to the active regions (occupied and virtual regions) is made by the carbon nanotube. The tweezer molecule is the perfect host for this carbon nanotube, because there is no electronic interaction between them.

As in the previous case, the binding energy of the complex, with regard to the fragments was calculated as −2.56 eV//−58.79 kcal/mol. This is a little more negative when compared to the nanotube (5,5) complex. The dispersion interaction was calculated as −1.35 eV//−30.96 kcal/mol, due to its additional Van der Waals interactions between C—C atoms, with 17 carbon-carbon bonds and 3 carbon-hydrogen bonds. These interactions are shown in Fig. 11, the number of bonds has been determined based on the correspondent molecular graph and the number of bond critical points between the species involved (Fig. 11).

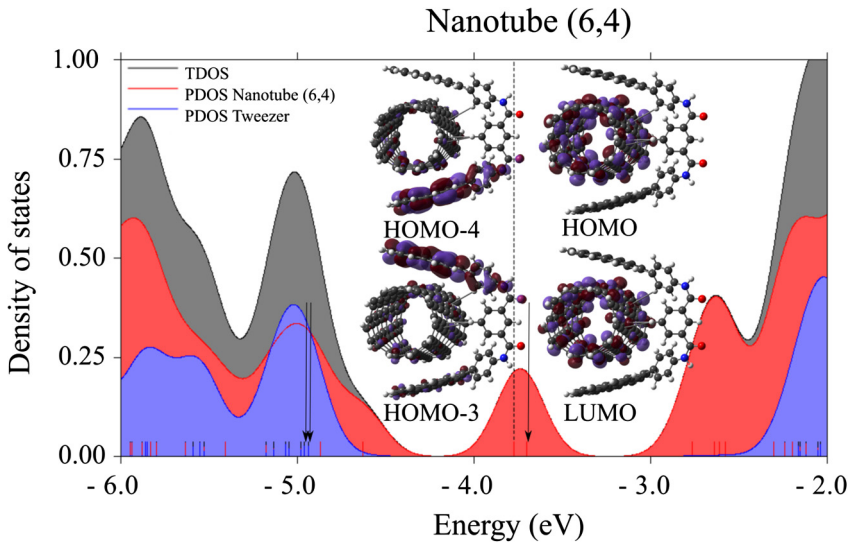

Fig. 10. Total and partial density of states and selected frontier orbitals of the scaffold complex (molecule **5**), dashed line indicates HOMO.

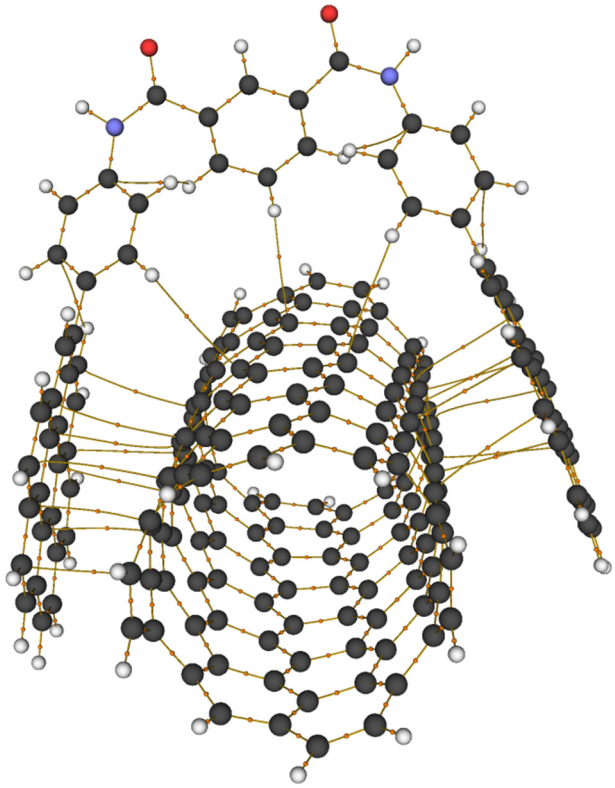

Fig. 11. QTAIM molecular graph of carbon nanotube (6,4) and molecular tweezer, orange dots are bond critical points. (For interpretation of the references to colour in this figure legend, the reader is referred to the web version of this article.)

The last description corresponds to the tweezer supporting nanotori. The nanotori is a proposed nanostructure which consists of a nanotube bent into a polyhedron, in the shape of a tire [49–51]. Nanotori structures can have different sizes and diameters as well as linear nanotubes; the one depicted here has an internal diameter which corresponds to a linear nanotube (3,3). It also has an internal diameter of 8.67 Å, an external one of 18.96 Å, and 216 carbon atoms.

The shape of the molecular tweezer supporting the nanotori (molecule **6**) is shown in Fig. 12. Notably, the union of the tweezer with the wheel is twisted a little in a clockwise direction and the nanotori is also slightly inclined towards the cleft of the tweezer and the arms of the tweezer are deviated a little away from the eclipsed conformation, so that overall the global conformation is not symmetric. The shortest distance between two carbon atoms from each structure is 4.8 Å.

There is a weak interaction between both fragments, which can be studied by focusing on its frontier molecular orbitals. The LUMO shows (Fig. 13) π contributions along the inner radius of the nanotori. The HOMO-LUMO gap is 2.453 eV//56.419 kcal/mol. This is larger than the complexes formed from nanotubes. HOMO and HOMO−1 are degenerated states; both orbitals show contributions in the jaws of the tweezer (Fig. 13). Similarly, HOMO−2 and HOMO−3 are degenerated states, extended over the jaws of the tweezer and with no contributions over the nanotori. The contributions of the nanotori appear 0.402 eV//9.25 kcal/mol deeper in energy, up to the HOMO−4, with π bonds extended over the entire nanotori.

In Fig. 13, it is possible to observe the density of states of the tweezer molecule with a nanotori as a guest. The gray line is the total density of states of the system, meanwhile the red line is the PDOS of the nanotori and the blue line is the PDOS of the tweezer molecule. In this system, there is a notable behavior, the nanotori also has a big gap in his PDOS, making a zero contribution in the total density of states. It is possible to observe that the HOMO orbital has a little contribution of the tweezer. As well, the LUMO orbital has a little of contribution of the nanotori, only, this phenomenon is seeing in the TDOS, in which the contribution of the LUMO is due the nanotori and the contribution of the HOMO is from the tweezer only. On the contrary of the carbon nanotube complexes, the tweezer introduces energy levels between the nanotori levels, thus reducing the gap.

Finally, dispersion interaction between the nanotori and the tweezer is calculated as −0.511 eV//−11.77 kcal/mol. In this case, the total binding energy was calculated as −0.37 eV//−8.61 kcal/mol. The electronic part of the energy is higher in energy than that of their components. Thus, the stabilization of the complex may be totally related to dispersion interaction. This interaction is smaller in comparison with the nanotube tweezer complex interaction. It can be understood in terms of the few Van der Waals contacts between carbon atoms. Likewise, the dispersion term was useful for predicting its geometry, as in this context, long range interactions have to be taken into account. In addition, according to its QTAIM molecular graph (Fig. 14), the weak interactions (and the correspondent energy) between the molecular tweezer and the nanotori can be related to five C—C bonds and three C—H bonds,

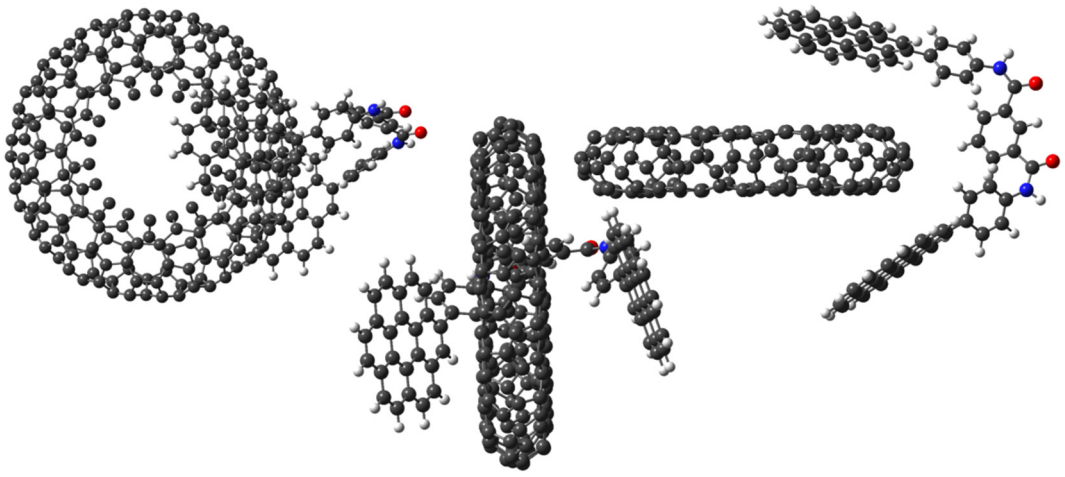

Fig. 12. Three views of the complex between the tweezer and the nanotori (molecule **6**).

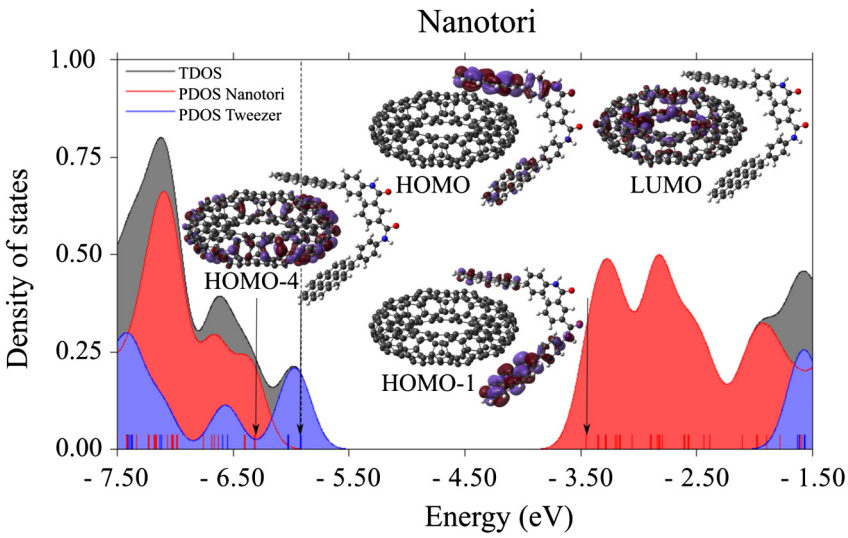

Fig. 13. Total and partial density of states and selected frontier orbitals of the scaffold complex (molecule **6**), dashed line indicates HOMO.

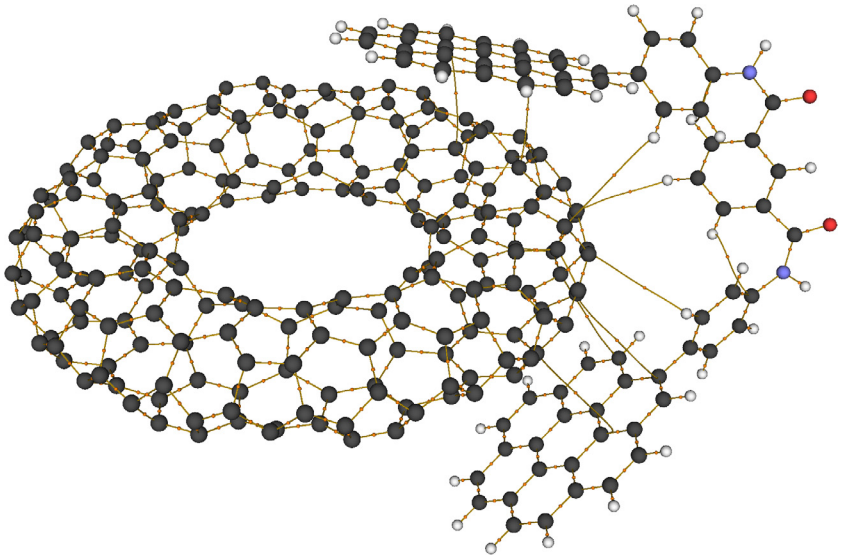

Fig. 14. QTAIM molecular graph of carbon nanotori and molecular tweezer, orange dots are bond critical points. (For interpretation of the references to colour in this figure legend, the reader is referred to the web version of this article.)

4. Conclusions

The molecular tweezer analyzed in the present paper can act as genuine tools, when trapping chemical species in different ways. Firstly, they can play the role of the decks of an organometallic metallocene trapping transition metal atoms, in large quantities. The analysis carried out with the Grimme's dispersion correction allow to estimate that there is a weak interaction between the molecular tweezer and the guest, as well as the molecular graph support these affirmations, displaying carbon-carbon and carbon-hydrogen bonds between the molecular tweezer and the guest species.

The molecular tweezer being studied could catch four Cr(0), forming an interesting semiconductor species which resembles metallocene molecules. In another context, the molecular tweezer can serve as scaffoldings that uphold narrow single walled nanotubes and carbon nanotori. The association between both moieties is achieved through dispersion forces, mainly those of the Van der Waals. The resultant complex retains the large majority of the physical and chemical characteristics of the nanotube, therefore it may be useful because the nanotube maintains its conductor behavior but is immobilized for practical purposes.

In particular, it should be seen that there is little electronic interaction between the tweezer molecule and the guest compound. With the density of states is possible to see how works the weak interaction between the guest and the molecular tweezer. Also, it demonstrates that the energy gap is completely determined by the guest species, exhibiting that the host species properties are remaining unchanged, even when there are inside of the molecular tweezers. It is possible to observe that this molecular tweezer is ideal to trap another molecules, like carbon nanotubes and carbon nanotori.

To sum up, with this molecular tweezer is possible to design a scaffold structure which can allow to trap organic molecules, regardless of the size of the guest. The guest remained unchained under this molecular tweezer.

Acknowledgement

The authors want to thank the kind help of Alberto López, Cain González, Alejandro Pompa, María Teresa Vázquez and Oralia Espinoza for technical help and Caroline Karslake for English style correction.

Funding: This work was supported by Dirección General de Asuntos del Personal Académico, Universidad Nacional Autónoma de México; grants from the projects DGAPA PAPIIT IN203816 and RN203816.

Appendix A. Supplementary material

Supplementary data associated with this article can be found, in the online version, at http://dx.doi.org/10.1016/j.comptc.2017.07.010.

References

[1] M. Hardouin-Lerouge, P. Hudhomme, M. Sallé, Molecular clips and tweezers hosting neutral guests, Chem. Soc. Rev. 40 (2011) 30–43.
[2] B. Legouin, M. Gayral, P. Uriac, J.-F. Cupif, N. Levoin, C. Toupet, P. van de Weghe, Molecular tweezers: synthesis and formation of host-guest complexes, Eur. J. Org. Chem. 5503–5508 (2010).
[3] J. Leblond, A. Petitjean, Molecular tweezers: concepts and applications, ChemPhysChem. 12 (2011) 1043–1051.
[4] F.-G. Klárner, B. Kahlert, Molecular tweezers and clips as synthetic receptors. Molecular recognition and dynamics in receptor-substrate complexes, Acc. Chem. Res. 36 (2003) 919–932.
[5] S.C. Zimmerman, C.M. VanZyl, G.S. Hamilton, G.S., Rigid molecular tweezers. Preorganized hosts for electron donor-acceptor complexation in organic solvents, J. Am. Chem. Soc. 111 (1989) 1373–1381.
[6] L.J. D'Souz, U. Maitra, Design, synthesis and evaluation of bile acid-based molecular tweezers, J. Org. Chem. 61 (1996) 9494–9502.
[7] T. Han, C.-F. Chen, A triptycene-based bis(crown ether host): Complexation with both paraquat derivatives and dibenzylammonium salts, Org. Lett. 8 (2006) 1069–1072.
[8] Ch. Mak, Unraveling base stacking driving forces in DNA, J. Phys. Chem. B 120 (2016) 6010–6020.
[9] A. Anderson, F. Yang, L. Cao, H.L. Mohammed, J. Meziani, Y.P. Sun, Tethered anthracene pair as molecular tweezers for post-production separation of single-walled carbon nanotubes, Chem. Phys. Lett. 657 (2016) 190–194.
[10] M.R. Axet, O. Dechy-Cabaret, J. Durand, M. Gouygou, P. Serp, Coordination chemistry on carbon surfaces, Coord. Chem. Rev. 308 (2016) 236–345.
[11] J. Kessler, M. Jakubek, B. Dolensky, P. Bour, Binding energies of five molecular pincers calculated by explicit and implicit solvent models, J. Comp. Chem. 33 (2012) 2310–2317.
[12] J. Antony, R. Sure, S. Grimme, Using dispersion-corrected density functional theory to understand supramolecular binding thermodynamics, Chem. Comm. 51 (2015) 1764–1774.
[13] E.M. Perez, N. Martin, Molecular tweezers for fullerenes, Pure Appl. Chem. 82 (2010) 523–533.
[14] P.A. Denis, F. Iribarne, Buckycatcher polymer versus fullerene-buckycatcher complex: Which is stronger, Inter. J. Quant. Chem. 115 (2015) 1668–1672.
[15] Y. Zhao, D.G. Truhlar, Computational characterization and modeling of buckyball tweezers: density functional study of concave-convex π—π interactions, PhysChemChemPhys 10 (2008) 2813–2818.
[16] J. Graton, B. Legouin, F. Besseau, P. Uriac, J.-Y.L. Questel, P. van de Weghe, D. Jacquemin, Molecular tweezers in host-guest complexes: a computational study through a DFT-D approach, J. Phys. Chem. C 116 (2012) 23067–23074.
[17] J. Graton, J.-Y.L. Questel, B. Legouin, P. Uriac, P. van de Weghe, D. Jacquemin, A DFT-D evaluation of the complexation of a molecular tweezer with small aromatic molecules, Chem. Phys. Lett. 522 (2012) 11–16.
[18] A. Ambrosetti, D. Alfé, R.A. DiStasio Jr., A. Tkatchenko, Hard numbers dor large molecules: toward exact energetic for supramolecular systems, J. Phys. Chem. Lett. 5 (2014) 849–855.
[19] M. Huhtala, A. Kuronen, K. Kaski, Carbon nanotube structures: molecular dynamics simulations at realistic limit, Comp. Phys. Comm. 146 (2002) 30–37.
[20] M.A. Herranz, C. Ehli, M. Campidelli, G.I. Gutierrez, K. Hug, K. Ohkubo, S. Fukuzumi, M. Prato, N. Martin, D.M. Guldi, Spectroscopic characterization of photolytically generated radical ion pairs in single wall carbon nanotubes bearing surface-inmobilized tetrathiafulvalenes, J. Am. Chem. Soc. 130 (2008) 66–73.
[21] C. Ehli, D.M. Guldi, M.A. Herranz, N. Martin, S. Campidellici, M. Prato, Pyrene-tetrathiafulvalene supramolecular assembly with different types of carbon nanotubes, J. Mater. Chem. 18 (2008) 1498–1503.
[22] D.A. Case, T.A. Darden, T.E. Cheatham III, C.L. Simmerling, J. Wang, R.E. Duke, R. Luo, R.C. Walker, W. Zhang, K.M. Merz, B. Roberts, B. Wang, S. Hayik, A. Roitberg, G. Seabra, I. Kolossváry, K.F. Wong, F. Paesani, J. Vanicek, J. Liu, X. Wu, S.R. Brozell, T. Steinbrecher, H. Gohlke, Q. Cai, X. Ye, J. Wang, M.-J. Hsieh, G. Cui, D.R. Roe, D.H. Mathews, M.G. Seetin, C. Sagui, V. Babin, T. Luchko, S. Gusarov, A. Kovalenko, P.A. Kollman, AMBER 11, University of California, San Francisco, 2010.
[23] J. Wang, R.M. Wolf, J.W. Caldwell, P.A. Kollman, D.A. Case, Development and testing of a general amber force field, J. Comp. Chem 25 (2004) 1157–1174.
[24] M. Valiev, E.J. Bylaska, N. Govind, K. Kowalski, T.P. Straatsma, H.J.J. Van Dam, D. Wang, J. Nieplocha, E. Aprà, T.L. Windus, W.A. De Jong, NWChem: a comprehensive and scalable open-source solution for large scale molecular simulations, Comput. Phys. Commun. 181 (9) (2010) 1477–1489.
[25] M.J. Frisch, G.W. Trucks, H.B. Schlegel, G.E. Scuseria, M.A Robb, J.R. Cheeseman, G. Scalmani, V. Barone, B. Mennucci, G.A. Petersson, et al. Gaussian 09, Revision, 2009.
[26] Y. Zhao, D.G. Truhlar, The M06 suite of density functionals for main group thermochemistry, thermochemical kinetics, noncovalent interactions, excited states and transition elements: two new functionals and systematic testing of four M06-class functionals and 12 other functionals, Theor. Chem. Acc. 120 (2008) 215–241.
[27] Y. Zhao, D.G. Truhlar, A new local density functional for main group termochemistry, transition metal bonding, termochemical kinetics and non-covalent interactions, J. Chem. Phys. 125 (2006) 194101.
[28] S. Grimme, J. Antony, S. Ehrlich, H.J. Krieg, A consistent and accurate ab initio parametrization of density functional dispersion correction (DFT-D) for the 94 elements H-Pu, Chem. Phys. 132 (2010) 54104.
[29] E.G. Hohenstein, S.T. Chill, C.D. Sherrill, Assessment of the performance of the M05–2X and M06–2X exchange-correlation functionals for noncovalent interactions in biomolecules, J. Chem. Theory Comput. 4 (2008) 1996–2000.
[30] S. Pakhira, K. Sen, C. Sahu, A.K. Das, Performance of dispersion-corrected double hybrid density functional theory: a computational study of OCS-hydrocarbon van der Waals complexes, J. Chem. Phys. 138 (2013), 164319:1–10.
[31] S. Pakhira, M. Takayanagi, M. Nagaoka, Diverse rotational flexibility of substituted dicarboxylate ligands in functional porous coordination polymers, J. Phys. Chem. C. 119 (2015) 28789–28799.
[32] T. Lu, F. Chen, Multiwfn: a multifunctional wavefunction analyzer, J. Comp. Chem. 33 (2012) 580–592.
[33] D. Seyferth, Bis(benzene)chromium. 2. Its Discovery by E. O. Fischer and W. Hafner and Subsequent Work by the Research Groups of E. O. Fischer, H. H. Zeiss, F. Hein, C. Elschenbroich, and Others, Organometallics 21 (2002) 2800–2820.
[34] N. Bensalem, B. Zouchoune, Coordination capabilities of anthracene ligand in binuclear sandwich complexes: DFT investigation, Struct. Chem. 27 (2016) 1781–1792.
[35] E.M. Perez, A.L. Capodilupo, G. Fernández, L. Sánchez, P.M. Viruela, R. Viruela, E. Orti, M. Bietti, N. Martín, Weighting non-covalent forces in the molecular recognition of C60, Relevance of concave–convex complementarity, 2008, 4567.
[36] X. Lu, Z. Chen, Curved Pi-conjugation, aromaticity, and the related chemistry of small fullerenes (<C60) and single-walled carbon nanotubes, Chem. Rev. 105 (10) (2005) 3643–3696.
[37] Y. Matsuda, J. Tahir-Kheli, W.A. Goddard III, Definitive band gaps for single-wall carbon nanotubes, J. Phys. Chem. Lett. 1 (19) (2010) 2946–2950.
[38] V. Meunier, L. Henrard, Ph. Lambin, Energetics of bent carbon nanotubes, Phys. Rev. B 57 (1998) 2586–2591.
[39] L. Chico, M.P. López Sancho, M.C. Muñoz, Novel 0D Devices: Carbon-Nanotube Quantum Dots, in: D. Reguera, J.M. Rubí, G. Platero, L.L. Bonilla (Eds.), Statistical and Dynamical Aspects of Mesoscopic Systems. Lecture Notes in Physics, vol. 547, Springer, Berlin, Heidelberg.
[40] H.F. Bettinger, Effects of finite carbon nanotube length on sidewall addition of fluorine atom and methylene, Org. Lett. 6 (5) (2004) 731–734.
[41] X. Wang, Q. Jiang, W. Xu, W. Cai, Y. Inoue, Y. Zhu, Effect of carbon nanotube length on thermal, electrical and mechanical properties of CNT/bismaleimide composite, Carbon 53 (2013) 145–152.
[42] V.G. Chilkuri, S. Evangelisti, T. Leininger, A. Monari, The electronic structure of short carbon nanotubes: the effects of correlation, Adv. Cond. Matter Phys. 2015 (2015) 475890:1–14.
[43] H. Kurebayashi, M. Sakaguchi, T. Okajima, T. Haino, S. Usui, Y. Fukazawa, Molecular tweezers based in Dioxa [2,2]ortocyclophane skeleton, Tetrahedron Lett. 40 (1999) 5545–5548.
[44] M.O. Sinnokrot, E.F. Valeev, C.D. Sherrill, Estimates of the *Ab Initio* limit for π-π interactions: the benzene dimer, J. Am. Chem. Soc. 124 (2002) 10887–10893.
[45] M. Alonso, T. Woller, F.J. Martín-Martinez, J. Contreras-García, P. Geerlings, F. De Proft, Understanding the fundamental role of π/π, σ/σ, σ/π dispersion interactions in shaping carbon-based materials, Chem. Eur. J. 20 (2014) 4931–4941.
[46] I. Alkorta, F. Blanco, J. Elguero, J.A. Dobado, S.M. Ferrer, I. Vidal, Carbon. . .carbon weak interactions, J. Phys. Chem. A 113 (2009) 8387–8393.
[47] A. Sánchez-González, F.J. Martín-Martínez, J.A. Dobado, The role of weak interactions in lignin polymerization, J. Mol. Model. 23 (80) (2017) 1–10.
[48] C.H. Suresh, K. Remya, Intermolecular carbon–carbon, nitrogen–nitrogen and oxygen–oxygen non-covalent bonding in dipolar molecules, Phys. Chem. Chem. Phys. 17 (2015) 18380–18392.
[49] J. Liu, H. Dai, J.H. Hafner, D.T. Colbert, R. Smaley, Fullerene "crop circles", Nature 385 (1997) 780–781.
[50] C. Chuang, J. Guan, D. Witalka, Z. Zhu, B.-Y. Jin, D. Tomànek, Relative stability and local curvature analysis in carbon nanotori, Phys. Rev. B 91 (2015) 165433.
[51] I. Lázló, A. Rassat, P.W. Fowler, A. Graovac, Topological coordinates for toroidal structures, Chem. Phys. Lett. 342 (2001) 369–374.